THE *SIMCA* ALGORITHM FOR PROCESSING GROUND PENETRATING RADAR DATA AND ITS USE IN LANDMINE DETECTION.

Mr. Anand Sengodan and Dr. W. Paul Cockshott

Computer Vision and Graphics Group, School of Computing Science, University of Glasgow, Glasgow, G12 8QQ

ABSTRACT

The main challenge of ground penetrating radar (GPR) based land mine detection is to have an accurate image analysis method that is capable of reducing false alarms. However an accurate image relies on having sufficient spatial resolution in the received signal. But because the diameter of an AP mine can be as low as 2cm and many soils have very high attenuations at frequencies above 3GHz, the accurate detection of landmines is accomplished using advanced algorithms. Using image reconstruction and by carrying out the system level analysis of the issues involved with recognition of landmines allows the landmine detection problem to be solved. The *SIMCA* ('*SIM*ulated *C*orrelation *A*lgorithm') is a novel and accurate landmine detection tool that carries out correlation between a simulated GPR trace and a clutter[1] removed original GPR trace. This correlation is performed using the *MATLAB*® processing environment. The authors tried using convolution and correlation. But in this paper the correlated results are presented because they produced better results. Validation of the results from the algorithm was done by an expert GPR user and 4 other general users who predict the location of landmines. These predicted results are compared with the ground truth data.

Index Terms – Ground Penetrating radar(GPR), Finite-difference-time-domain(FDTD) simulation, landmines, correlation, clutter.

1. INTRODUCTION

Inspite of the fact that record funding was given by various government organizations in 2011, there are vast number of landmines still uncleared. This is because of the fact that plastic landmines and Improvised explosive devices(IEDs) pose a challenge to the deminer. According to the Landmine Monitor 2011 report[2] at least 72 states and seven disputed areas around the world are infested with over 100 million landmines.

Metal detectors are unable to detect plastic landmines and hence the importance of GPR can be realised. But GPR data suffer from clutter. Clutter detected by the GPR includes many components: cross talk from transmitter to receiver antenna, initial ground reflection and background resulting from scatterers within the soil [12, 13, 14]. A clutter removal technique developed by Sengodan and Javadi [2] is used to remove the clutter. The theory of waveguides developed by [7, 8, 12] is important in understanding the principles of GPR and to develop the *SIMCA* algorithm.

The use of the *GprMAX2D v1.5* developed by Giannopoulos [1] which uses the finite-difference time-domain method (FDTD) to solve Maxwell's equations; enabled the replication of the original test setup, to better understand the test situation and to quickly derive the correlation kernel. The simulation gives the ideal trace of a point reflector placed in the same soil conditions as the experimental setup. The actual process involved in deriving the kernel from the simulated result is by the selection of a rectangular area covering the hyperbolic shape (this is because the presence of landmines is depicted by distinctive hyperbolic shapes) and then normalisation of this signal in *MATLAB*®.

Then using the *MATLAB*® processing environment the clutter removed GPR image is correlated with the correlation kernel to produce a correlated image.

The validation of the algorithm was done using an expert and several ordinary users because often in a daily landmine clearing situation, humans are involved in the interpretation of the results. Also the size of the validation data is acceptable because it uses 125 data sources and using such a test size is in accordance with current research [4].

The proposed algorithm is shown in Figure 1.

The *SIMCA* algorithm was tested on data given to the authors by researchers who conducted GPR experiments in a sandbox using a robotic scanner [3].

The *SIMCA* algorithm has been used to process GPR data and to use it to locate foundations in demolished buildings [5].

1.1. GprMax2D v1.5 for simulation of GPR data

The aim of the GPR simulation was to generate the correlation kernel. One approach of simulating a GPR would be to use Maxwell's equations and the recieved voltage representing an A-scan[3] and to mathematically calculate

[1] Clutter is all the reflections that do not originate from the target but from the background.

[2] http://www.the-monitor.org

[3] The A-scan is a time-amplitude plot and represents a single pulse return with the GPR antenna at a specific location above the ground.

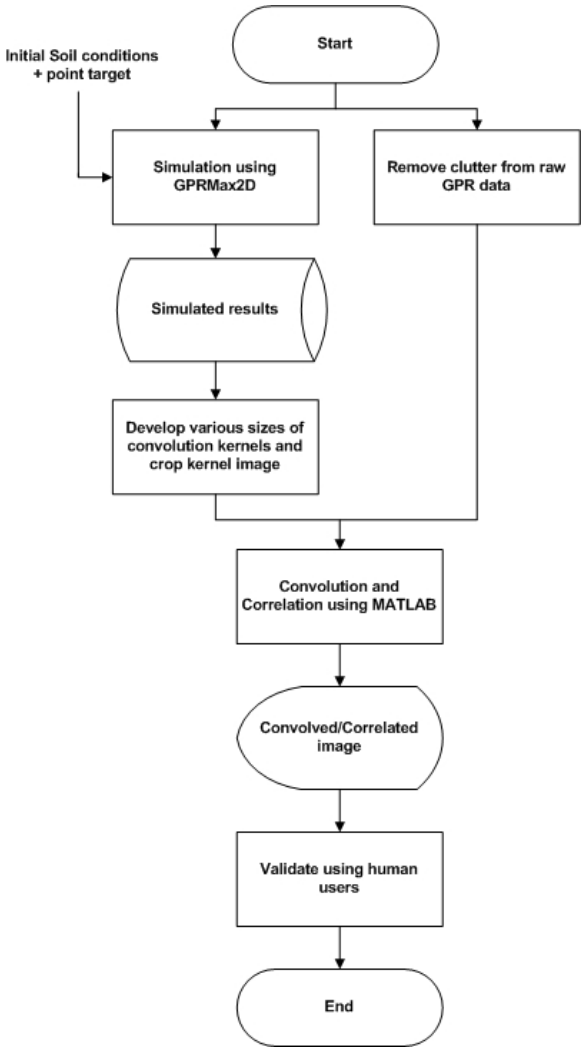

Fig. 1. *The proposed SIMCA algorithm. The* SIMCA *algorithm proceeds firstly by carrying out processing via two parallel streams. The first of this parallel stream involves carrying out the simulations using the simulation software. Various sizes of correlation kernels were then designed. The other parallel stream removes clutter from the raw GPR data. This clutter is removed before the processing of the results. Convolution and correlation were then carried out using the correlated kernel and the clutter removed GPR data. In this paper we present the correlated results because they produced better results than convolution. The validation is done using a human expert and four other non-expert users. Validation using a human subject is better than a automatic programme because it replicates the scenario in the field.*

the point spread function of the point reflector by carrying out transformations and simplifications.

But for this study, the *GprMax2D V1.5* electromagnetic simulator was used. The program basically solves Maxwell's equations using the FDTD method. The FDTD approach to the numerical solution of Maxwell's equations is to discretize both the space and time continua. Thus the discretization spatial Δx, Δy, Δz and temporal Δt steps play a very significant role, since the smaller they are the closer the FDTD model is to a real representation of the problem. However, the values of the discretization steps always have to be finite, since computers have a limited amount of storage and finite processing speed. Hence, the FDTD model represents a discretized version of the real problem and is of limited size. The building block of this dicretization grid is the Yee cell named after Kane Yee [6] who pioneered the FDTD method. Figure 2 illustrates the 3D FDTD Yee cell which is used by the program.

The simulation program takes a data file as input containing soil conditions, domain size, discretization step, time window, details of the buried object(in this case a spherical object), details of the GPR and the location of the transmitter and receiver in the co-ordinate system. For running the simulations, a 0.025m radius sphere buried at the depths corresponding to the target burial depth at the lab was used. This closely resembled the test condition used in acquiring of the landmine data and produced a centralised kernel which was large and included a large proportion of the hyperbola sidelobes. The hyperbola sidelobes cause better localisation of the data and hence the target can be easily distinguished. Then the pro-

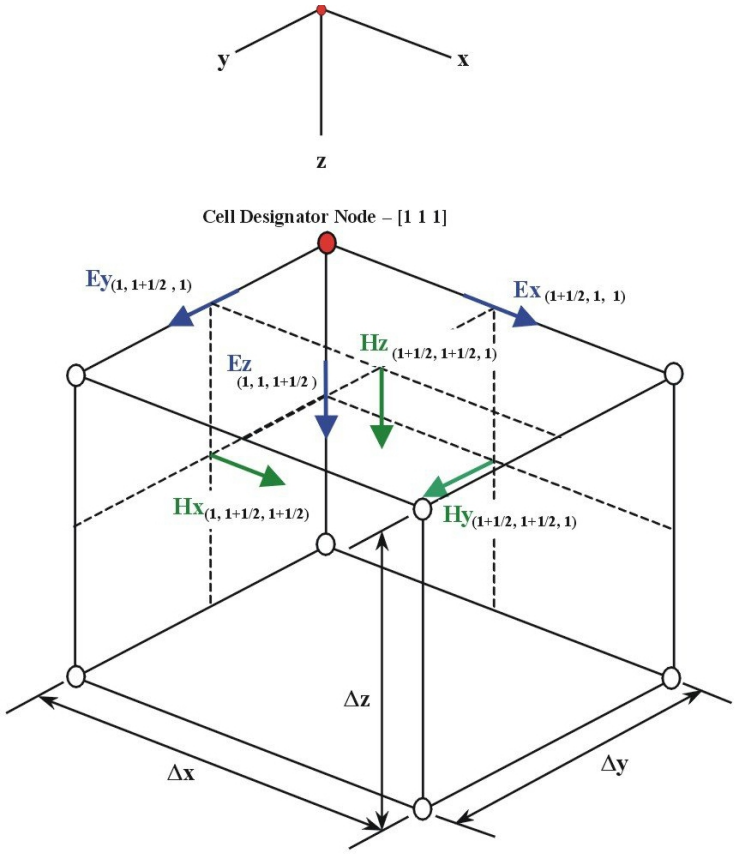

Fig. 2. *The 3D FDTD Yee Cell from [6].*

gram runs the simulation and produces a geographical file describing the original test conditions input into the simulation and the output file containing the simulated data.

This simulated data is then imported into *MATLAB*® for further processing and to carry out the convolution and correlation.

1.2. Normalization of the raw data and the correlation kernel

Statistical normalization helps in normalizing the raw and the correlation kernels for further processing. In order to carry out normalisation the following statistical normalization technique was used:

$$Z_{norm} = \frac{A - \mu}{S}$$

where Z_{norm} is the normalised signal; A is the original signal; μ is the mean; S is the standard deviation and the $(A\text{-}\mu)$ is carried over the entire matrix of data.

1.3. Convolution and Correlation

Then using the following *MATLAB*® function the clutter removed GPR data and the correlation kernel were correlated:

$$C = imfilter(normala, normalb, 'function')$$

where C is the final convolved or correlated image; $normala$ is the normalized clutter removed GPR data, $normalb$ is the normalized kernel and $'function'$ is $'conv'$ for convolution or $'corr'$ for correlation.

2. RESULTS

The algorithm was initially tested for the simulated data and it produced promising results. The algorithm was able to locate the spherical object at the correct depth.

Various visualization techniques [9, 10, 11, 12] were used to present the data to mine clearing personnel. The following visualization techniques were useful:

- Correlation to a false colour.
- Non-linear operation of squaring and raising to a higher power of the brightness values.
- Mesh developed in *MATLAB*®.

From the above visualization techniques used the generated mesh (Figure 3[C]) shows the peak clearly but it is less easy to localise the peak in this representation than it is in Figure 3[B]. From Figure 3[B] the peak value is clearly shown and this shows the location of the landmine. The visualization technique used in Figure 3[D] is more easy to identify the peak value in comparison to the other two techniques. Also the horizontal line that runs continuously across the images in Figures 3[B] and 3[D] is

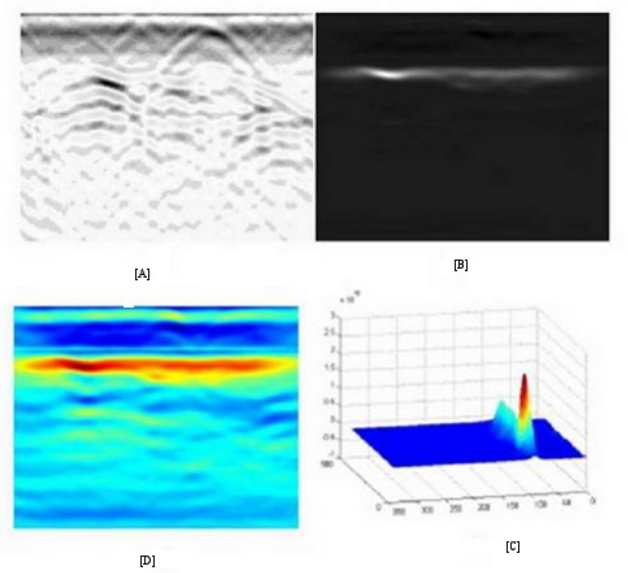

Fig. 3. *Clockwise from left- [A]: Clutter removed GPR image; [B]: Correlated image with brightness raised to power of 3; The non-linear operation of raising to the power identifies the correct peak area; [C]: Mesh generated with MATLAB; [D]: False color representation of the correlated image which has not been raised to power of 3.*

because there is a Bullet, a PMN mine, a metal ring, and a PMA-3 mine all buried at the same depth. This shows a horizontal line as the peak values of the reflections are continuous in nature and extend along the objects. Another reason is because the experiment is carried out in a laboratory, the soil has not been properly compacted and appears as a horizontal line.

Results are also surprisingly good considering the profile of the relevant detail in the hyperbolic kernel is more horizontal than vertical.

2.1. Results for the rest of the data

In this paper, presentation of the remainder of the data is done using tabular format showing the estimated depths of the targets in the setup along with the actual depth of burial of these targets for 10 of the data samples.

The human subjects were asked to mark the location of the landmine on an printed image of Figure 3[B] and then on the basis of the radar and soil equations, the depths were estimated. Therefore the depths were the estimated depths on the basis of the located mines. An expert user of GPR was first used to estimate the location of the object by giving then the correlated image with the brightness raised to the power of 3. The experiment was repeated for a large dataset and produced similar results, but this paper summarises the main results.

From the results, presented in Table 1, it can be seen that the expert is able to locate the landmines and the highest percentage error is only 18%. This is not bad for initial results. Furthermore from the results it is quite evident that the correlated results are accurate when compared to the actual ground truth. The results obtained were also better at lower and middle depths. Apparently at depths close to the surface, there is strong interference of mine clutter in the mine backscatter. Similarly with the increase in depth, there is damping of the electrical field and therefore a corresponding decrease in backscatter from the mine and increase in the soil clutter.

Therefore it may be concluded that the proposed technique is capable of predicting the depths correctly subject to the accuracy of the observed backscatter and the content of soil clutter in it.

2.2. Validation of the results

The authors then presented the correlated data to 4 other people who have never seen GPR data. There were 25 images presented to each of the subjects and Table 3 shows the actual depths, estimated depths, actual scan positions and the estimated scan positions for four subjects. It is to be noted that although there were 25 images presented to the subjects, the table gives the results for 10 images. The users were again asked to identify the presence or absence of landmines by marking the correlated images with a pen showing where they felt the mines were located. These results were timed and then fed into the Microsoft Access database.

From Table 3 the non-experts found the landmines to acceptable degrees of accuracy. It is to be noted in Tables 3 and 4 that when the user was not able to identify the presence of a landmine a dash is used and the mean and standard deviation are worked out on the basis that the concerned dataset was not used to get meaningful results. From Table 3, it is evident that the standard deviation for the actual and those estimated on the basis of the predictions from the users are close to each other showing a promise in the results. Furthermore the standard deviations are small indicating the variation from the mean is small and hence the results are accurate.

Also the systematic bias is not bad compared to the extreme conditions depicted. These have been corrected and are in close proximity to actual results. In any experiment systematic bias does exist, but it is important that the final data is corrected to take care of the systematic bias. The error both in depth (y) and in horizontal position (x) are given. The horizontal error is obviously also important since it is important to know where to dig to find the mine. Then splitting is done using the calculated values from Table 3 and is shown in Table 4. The splitting is done proportionately in the x and y directions.

It is positive to note from Table 2 that the 'False Negative' rates are low because this is really important in landmines as it is not mission critical to overestimate that a mine is present but missing out the presence of a landmine is dangerous. Also from Table 2, it can be seen that the results for both the expert and the non-expert are promising and have a low false alarm rate. The highest false alarm rate is only 19% which is quite good in comparison to re-

sults obtained by other authors using different techniques.

From the chart in Figure 4, the actual depth as shown by series 1 is plotted as both a linear and as a scatter plot and the series 2, 3, and 4 are the estimated depths on the basis of the subjects predictions of the where the mines were located. The chart shows that the users were able to predict the location of landmines to acceptable degrees of accuracy as indicated by the closeness of the predicted and the actual depths.

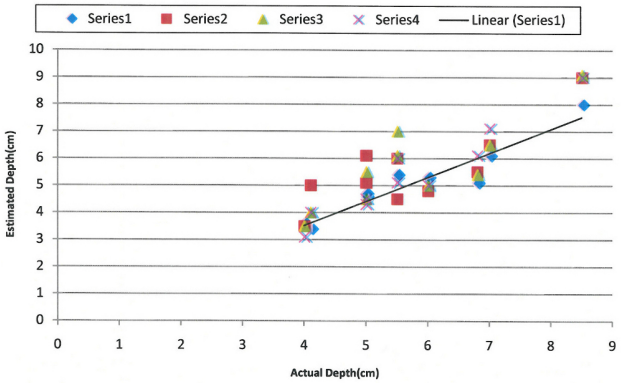

Fig. 4. *Error plot of predicted depth versus actual depth. Series 1 indicates the expert user and series 2-4 indicates the non expert users. Also the linear label is the trend line analysis for the expert user.*

3. CONCLUSION

The proposed ***SIMCA*** algorithm is therefore a novel method of helping the de-mining personnel predict the location of landmines with acceptable degrees of accuracy.

The results are great considering the profile of the relevant detail in the hyperbolic kernel is more horizontal than vertical. Also expert and non-expert users were able to predict mines to acceptable degrees of accuracy.

In order to improve the results, it would be necessary to repeat this process using a 3-D approach and apply convolution and correlation to the 3-D profiles of the data. Also further visualization techniques and OpenGL are going to be used. The algorithm is going to be tested on different data sources to see the effectiveness of the algorithm on a number of conditions and operating differences.

4. REFERENCES

[1] A. Giannopoulos, "GprMax software and manual," http://www.gprmax.org/.

[2] A. Sengodan, and A. Javadi, "Landmine detection using masks on ground penetrating radar images," *IRIS 2005*.

[3] Vrije Universiteit, "GPR experiments in a sandbox," Brussels, April 1999.

[4] I. Guyon, J. Makhoul, R. Schwartz and V. Vapnik, "What size test set gives good error rate estimates?," *AT&T Bell Labs memorandum BL0115540-951206-07, submitted to PAMI*, 1995.

[5] A. Sengodan, W. P. Cockshott and C. Cuenca-Garcia, "The SIMCA algorithm for processing Ground Penetrating Radar data and its use in locating foundations in demolished buildings," *2011 IEEE RadarCon Conference,* pp. 706-709, May 2011.

[6] K. S. Yee, "Numerical solution of initial boundary value problems involving Maxwell's equations in isotropic media," *IEEE Trans. on Ant. and Prop.*, Vol. 14, No. 3, pp. 302-307, 1966.

[7] L. Leonard, "Advanced theory of waveguides," *Wireless Engineer*, 1951.

[8] M. Dietrich, "Theory of dielectric optical waveguides," *Academic Press*, 1974.

[9] C. Ware, "Information visualization: perception for design," 2000.

[10] J.C. Russ, "The image processing handbook," 3rd edition, 1999.

[11] T. Pavlidis, "Algorithms for graphics and image processing," 1982.

[12] D. J. Daniels, "Ground Penetrating Radar: 2nd Edition," *IEE Radar, Sonar and Navigation Series 15*, 1982.

[13] L. Capineri, P. Grande, and J. Temple, "Advanced image processing technique for real time interpretation of Ground Penetrating Radar images," *IEEE Transactions*, vol. 9, pp. 51-59, 1998.

[14] D.J. Daniels, "Surface Penetrating Radar Image Quality," *MD'98 second international conference on the detection of abandoned land mines*, pp 68-72, Edinburgh, UK, 12-14 October 1998.

Table 1. *Rest of the results on the correlated data. In this table column 1 and column 2 are the estimated and actual depths in cm respectively and column 3 is the % error. In the below table the actual depth was the depth based on the ground truth and corresponds to the actual depth of the landmines. The estimated depths are those estimated by the expert user. The expert user is used to show the accuracy of the results. Once the expert user was used in the validation of the results non-expert users were used to validate the results.*

1	**2**	**3**	**1**	**2**	**3**	**1**	**2**	**3**	**1**	**2**	**3**
Bullet	Bullet	Bullet	PMN	PMN	PMN	Ring	Ring	Ring	PMA-3	PMA-3	PMA-3
4.7	5.0	6.0	4.3	5.1	15.6	4.8	4.6	-4.3	4.7	5.0	6.0
5.1	4.5	-13.3	5.1	4.8	-6.2	5.2	5.5	5.5	5.3	6.0	11.7
8.1	7.6	-6.6	8.2	8.5	3.5	8.1	7.8	-3.8	8.0	8.5	5.8
5.6	5.0	-12.0	5.5	5.0	-10.0	5.1	5.3	3.7	5.1	6.8	25.0
4.9	4.6	-6.5	4.8	4.6	-4.3	4.6	5.0	8.0	4.5	5.5	18.1
3.4	4.0	15.0	3.5	4.0	12.5	3.8	3.6	-5.6	3.6	4.0	10.0
4.9	4.6	-6.5	4.8	4.6	-4.3	4.7	4.5	-4.4	4.6	5.0	8.0
5.4	5.6	3.6	5.6	6.0	6.7	5.5	5.6	1.8	5.4	5.5	1.8
3.2	2.9	-10.3	3.3	3.1	-6.5	3.1	2.9	-6.9	3.4	4.1	17.1
6.7	5.9	-13.6	6.6	6.8	2.9	6.3	6.8	7.4	6.1	7.0	12.9

Table 2. *False positive and False negative rates. In the below table the +ve column is the false positive and the -ve column is the false negative. The setup had a total of 21 mines and the expert('Expert') and non-expert('Non') users were asked to identify the location of the mines and the below results were collated.*

Total Mines	Expert	Expert	Non1	Non1	Non2	Non2	Non3	Non3	Non4	Non4
	+ve	-ve	+ve	-ve	+ve	-ve	+ve	-ve	+ve	-ve
21	3	0	4	1	3	1	4	0	3	0

Table 3. *In the below table X1 is the systematic bias on the depth and Y1 is the systematic bias on the scan position (horizontal position). The x-position is the scan position, M1 is the mean error and S2 is the standard deviation. Also 'Act.' is the actual and 'Est.' is the estimated. The depths and scan positions are in centimetres.*

	1	**2**	**3**	**4**			**1**	**2**	**3**	**4**	
Act. depth	Est. depth	Est. depth	Est. depth	Est. depth	X1	Act. pos.	x-pos.	x-pos.	x-pos.	x-pos.	Y1
5.0	4.7	5.1	5.5	4.3	0.1	7.0	6.2	7.8	8.0	6.8	-0.2
6.0	5.3	4.8	5.0	-	1.1	15.6	14.8	16.1	15.1	-	0.3
8.5	8.0	9.0	9.1	9.0	3.6	4.3	3.1	5.1	4.5	4.1	0.1
6.8	5.1	-	5.4	6.1	1.9	20.7	19.4	-	21.1	18.6	1.0
5.5	4.5	6.0	7.0	5.1	0.6	8.5	7.8	9.0	8.1	7.9	0.3
4.0	3.6	3.5	3.5	3.1	-0.9	11.5	12.0	10.9	11.1	12.0	0.0
5.0	4.6	6.1	4.5	4.5	0.1	3.2	2.9	2.1	3.8	2.9	0.3
5.5	5.4	4.5	6.1	6.0	0.6	4.8	5.0	4.7	3.9	4.1	0.4
4.1	3.4	5.0	4.0	-	-0.8	6.5	6.8	7.0	5.8	-	0.0
7.0	6.1	6.5	6.5	7.1	2.1	5.6	5.1	4.9	5.6	6.0	0.2
M1					0.8						0.2
S2					1.4						0.32

Table 4. *The mean error is split in the x and y directions. The x direction is horizontal position and the y direction is the depth. Again the depths and scan positions are in centimetres.*

1	**1**	**1**	**1**	**2**	**2**	**2**	**2**
y dir.	y1	x dir.	x1	y dir.	y2	x dir	x2
4.7	5.5	6.2	6.4	5.1	5.9	7.8	8.0
5.3	6.1	14.8	15.0	4.8	5.6	16.1	16.3
8.0	8.8	3.1	3.3	9.0	9.8	5.1	5.3
5.1	5.9	19.4	19.6	-	-	-	
4.5	5.3	7.8	8.0	6.0	6.8	9.0	9.2
3.6	4.4	12.0	12.2	3.5	4.3	10.9	11.1
4.6	5.4	2.9	3.1	6.1	6.9	2.1	2.3
5.4	6.2	5.0	5.2	4.5	5.3	4.7	4.9
3.4	4.2	6.8	7.0	5.0	5.8	7.0	7.2
6.1	6.9	5.1	5.3	6.5	7.3	4.9	5.1